An X-ray study of the physiological-temperature form of hen egg-white Lysozyme at 2Å resolution

Jean Berthou, Alain Lifchitz, Pete Artymiuk, Pierre Jollès

Proc. R. Soc. Lond. B **217**, 471–489 (1983)
Printed in Great Britain

An X-ray study of the physiological-temperature form of hen egg-white lysozyme at 2 Å† resolution

BY J. BERTHOU[1]‡, A. LIFCHITZ[1], P. ARTYMIUK[2] AND P. JOLLÈS[3]

[1]*Laboratoire de Minéralogie–Cristallographie associé au C.N.R.S., Université Pierre et Marie Curie, 4 place Jussieu, F 75230 Paris Cedex 05, France*

[2]*Laboratory of Molecular Biophysics, Zoology Department, South Parks Road, Oxford OX1 3PS, U.K.*

[3]*Laboratoire des Protéines, Universités de Paris V et VI (I.N.S.E.R.M. U-116 and C.N.R.S., E.R. 102), 45 rue des Saints-Pères, F 75270 Paris Cedex 06, France*

(*Communicated by Sir David Phillips, Sec.R.S. – Received 2 August* 1982)

The structure of the high-temperature orthorhombic form of hen egg-white lysozyme has been determined at 2.0 Å resolution. Initial images of the molecule were obtained at 6.0 Å resolution both by double isomorphous replacement and by molecular replacement with use of the known structure of the room-temperature tetragonal lysozyme. The initial model thus obtained ($R = 0.52$ at 6.0 Å) was refined first as a rigid body at 6.0 Å and then by restrained least squares at 2.5 Å and later at 2.0 Å resolution. The final model ($R = 0.23$ at 2.0 Å) was compared with that of the tetragonal form: the structures are very similar with a root mean square difference in superimposed α-carbon coordinates of 0.46 Å. There are, however, differences which are caused by a crystal contact involving the upper part of this active site in the high-temperature orthorhombic form. Because of this, residues Trp 62 and Pro 70 are much better ordered than in the tetragonal form, where they are exposed to solvent. These differences can partly explain the difficulty of inhibitor-binding in high-temperature orthorhombic crystals, but do not seem to reflect the particular behaviour of lysozyme in solution at high temperature.

1. INTRODUCTION

Hen egg-white lysozyme (EC 3.2.1.17) is known to crystallize in a great variety of forms depending upon the nature of the precipitating salt and the choice of pH (Steinrauf 1959; Imoto *et al.* 1972). Of these, many have already been studied by X-ray techniques. The structure of the molecule in the tetragonal form has been solved to a resolution of 2 Å (Blake *et al.* 1965, 1967*a*). Its complexes with saccharides provided a basis for approaching the nature of catalytic properties of the protein and enabled Blake *et al.* (1967*b*) to propose a mechanism of action. The triclinic as well as the monoclinic and the low-temperature orthorhombic forms have also been the subject of extensive investigations (Joynson *et al.* 1970; Hodson *et al.* 1974; Moult *et al.* 1976; Hogle *et al.* 1981; Artymiuk *et al.* 1982). All these

† 1 Å = 10^{-10} m.

‡ To whom all correspondence should be addressed.

studies showed clearly that lysozyme has essentially the same conformation in these forms ($T < 20$ °C).

In 1972, Jollès & Berthou noticed that tetragonal crystals were unstable above 25 °C and especially at physiological temperatures (37–40 °C): under the influence of temperature alone they transformed into stable orthorhombic crystals. Later on it became clear (Berthou & Jollès 1974, 1978) that the other forms obtained at low temperature were able to transform into this same orthorhombic form, whatever the initial conditions of crystallization had been, the only difference being the transition point.

To this thermodependence of lysozyme crystallization there correspond particular properties in solution. Evidence for a specific temperature-dependent conformational transition between 20 and 30 °C was obtained by means of ^{13}C-nuclear magnetic resonance spectroscopy (Cozzone *et al.* 1975); a decrease in the affinity of lysozyme for *N*-acetylglucosamine was noted at neutral pH above the transition temperature (25 °C), when this sugar was known to be a strong inhibitor at 20 °C (Jollès *et al.* 1975). Evidence in favour of the existence of a structural transition in lysozyme, which does not involve denaturation, has also been provided by the finding of a sharp break in the Arrhenius plot at 25 °C: a pH dependence of this temperature-induced rearrangement was observed, which suggests a possible involvement of some carboxylic groups in the transition (Saint-Blancard *et al.* 1977). As some importance has already been attributed to these carboxylic groups in the inhibitory action of *N*-acetylglucosamine at *low* temperature, Saint-Blancard *et al.* (1979) decided to reinvestigate the action of this sugar at 40 °C (physiological temperature for birds) and at different values of pH; inhibitor-insensitive lysozyme forms were thus characterized. Finally it was recently determined (Saint-Blancard *et al.* 1981) that, in the pH range 6.7–8.6 frequently used in experiments involving lysozyme, the pH optimum of lysis of *Micrococcus luteus* cells at low ionic strength (0.02–0.05) by the high-temperature form was 1–2 units lower than that by the low-temperature form. All these experiments suggested the existence of two different temperature-induced ranges in each of which lysozyme behaves differently, possibly because of different conformations. These were called the A and B forms (low- and high-temperature forms, respectively).

Two independent 6 Å maps of the structure of these high-temperature orthorhombic crystals were obtained by means of double isomorphous replacement (Berthou *et al.* 1977) and molecular replacement (Harada *et al.* 1981). These maps showed that the molecular conformation was generally the same as in the low-temperature form and that the upper part of the active site was involved in a crystal contact, which possibly explains why inhibitors such as *N*-acetylglucosamine and chitobiose were prevented from binding to the molecule in these crystals.

It was clear that higher resolution was needed before any serious comparisons with other crystal forms were attempted. Once approximate coordinates from molecular replacement were available for orthorhombic crystals, the molecular model was refined in the usual crystallographic sense against data from these crystals.

2. Materials and methods

(*a*) *Crystallization*

Three commercial samples of hen egg-white lysozyme were used and all produced the same high-temperature crystals (lysozyme six times crystallized, from Miles; lysozyme six times crystallized, from Seikagaku; lysozyme crystallized at Boehringer). Our crystallizations were done at a constant temperature of 40 °C as follows: to 50 mg of lysozyme dissolved in 0.5 ml of water were added 0.0625 ml of 0.2 M acetate buffer, pH 4.7, and 0.1875 ml of water; after centrifugation if necessary, 0.75 ml of a 100 mg ml^{-1} NaCl solution was added to the clear supernatant (Jollès & Berthou 1972). The crystals are orthorhombic ($P2_12_12_1$, $Z = 4$, $a = 56.4$ Å, $b = 73.8$ Å, $c = 30.4$ Å, $\alpha = \beta = \gamma = 90°$).

(*b*) *Data collection and processing*

The two native data sets, 6.0 and 2.0 Å, were collected with the 'stepscan' routine on a Philips PW 1100 single-crystal automatic diffractometer. A crystal of dimensions 0.50 mm × 0.50 mm × 0.30 mm was used and data were measured to 2.0 Å resolution ($\theta_{max} = 22°$), yielding 9418 independent reflexions. The radiation damage was monitored by measuring each of three standard reflexions every hour. These three reflexions were chosen to be in a medium resolution range. The mean reduction of intensity was 10 % over the period of the data collection. This decrease was practically linear with time.

Intensities were corrected for Lorenz and polarization factors and for irradiation damage and absorption, the last by means of the Agnost program (Coppens *et al.* 1965). Mean discrepancies between equivalent intensities were, after correction, close to 4 %.

In addition, low-resolution data for two heavy atom derivatives and 2.5 Å native data collections were measured on a Hilger and Watts Y230 four-circle diffractometer converted for five-circle five-counter use (Banner *et al.* 1977) and controlled by a Ferranti Argus computer. The diffractometer was mounted on a Philips PW 1130 X-ray generator fitted with an Elliott fine-focus X-ray tube running at 40 kV, 30 mA. The diffraction intensities were measured with a proportional counter and output to magnetic tape in the ordinate analysis mode (Watson *et al.* 1970). The two heavy atom data sets consisted of Bijvoet pairs of reflexions (hkl, $hk\bar{l}$) to 6 Å. The native set comprised two equivalents of reflexions. Those lying between 20 and 6 Å were measured in single counter symmetrical-A mode. The reflexions that were accessible in flat-cone geometry (with a c* mount) were measured in five-counter mode, and then the blind region to 2.5 Å was filled in by using single counter symmetrical-A geometry. During each data collection, standard reflexions were re-measured at intervals to monitor radiation damage and crystal slipping. A North *et al.* (1968) absorption curve was measured for each crystal and counter–counter scales were estimated for the native data.

Background, Lorenz polarization and absorption corrections were made on an I.C.L. 1906 A computer. The three data sets were internally merged and anomalous scattering information was extracted for the heavy atom derivative sets which were then scaled to the native set.

Patterson and Fourier maps were calculated by using Fast Fourier Transform programs. Refinement of heavy atom positions and occupancies was done by the F_{HLE} method of Dodson & Vijayan (1971).

TABLE 1

(a) Definition of symbols for heavy atom refinement

F_o observed structure factor amplitude
F_c calculated structure factor amplitude
F_P observed structure factor amplitude for native protein
F_{PH} observed structure factor amplitude for protein and heavy atom
F_H estimated structure factor amplitude for heavy atom alone
α_{FHLE} phase calculated using the lower estimate of F_H from isomorphous and anomalous differences (Dodson & Vijayan 1971)
α_{iso} phase of structure factor determined by isomorphous replacement (Blow & Crick 1959)
E_{iso}, E' total standard errors in the closure of the isomorphous and anomalous phase triangles

(b) Definition of symbols for molecular replacement

$\boldsymbol{h} \equiv (h, k, l)$ Miller indices of reflexion
$F_c(\boldsymbol{h})$ calculated molecular structure factor of the isolated model, in a hypothetical P_1 cell for the rotation function $R(\boldsymbol{\theta})$, and in the observed cell for the translation function $T(\boldsymbol{t})$
$\boldsymbol{\theta} \equiv (\theta_1, \theta_2, \theta_3)$ Eulerian angles triplet specifying the current orientation of the model
$\boldsymbol{\theta}_0$ Eulerian triplet corresponding to the best agreement, in orientation, between the model and the observed structure
$R(\boldsymbol{\theta}) \equiv \Sigma_{\boldsymbol{h}}\Sigma_{\boldsymbol{h}'}|F_m(\boldsymbol{h})|^2|F_o(\boldsymbol{h}')|^2 G_{\boldsymbol{h}\boldsymbol{h}'}(\boldsymbol{\theta})$ rotation function of Rossman & Blow (1962), which takes a maximum value for the best agreement in orientation between model and observed structure; $G_{\boldsymbol{h}\boldsymbol{h}'}(\boldsymbol{\theta})$ is an interference function.
$\boldsymbol{t} \equiv (t_x, t_y, t_z)$ fractional cell coordinates specifying the current position of the well oriented model ($\boldsymbol{\theta} = \boldsymbol{\theta}_0$) in the observed cell
$\boldsymbol{t}_0$ position of the model corresponding to the best agreement between the model and the observed structure
$F_c(\boldsymbol{h}, \boldsymbol{t})$ calculated structure factor, for $\boldsymbol{\theta} = \boldsymbol{\theta}_0$, of the observed structure
N number of asymmetric units in the observed crystal cell
$T(\boldsymbol{t}) \equiv N\Sigma_{\boldsymbol{h}}|F_m(\boldsymbol{h})|^2 \dfrac{\Sigma_{\boldsymbol{h}} F_o^2(\boldsymbol{h})|F_c(\boldsymbol{h}, \boldsymbol{t})|^2}{\Sigma_{\boldsymbol{h}} F_o^4(\boldsymbol{h})\Sigma_{\boldsymbol{h}}|F_c(\boldsymbol{h}, \boldsymbol{t})|^2}$ translation function of Harada *et al.* (1981), which takes a maximum value for the best agreement, in position, between the well oriented model and observed structure

(c) Refinement of heavy atom parameters (For definition of symbols, see table 1*a*.)

Over 100 attempts were made to find suitable heavy atom derivatives, but only two were found, both of them being uranyl compounds: $K_3UO_2F_5$ and $UO_2(CH_3COO)_2$. The diffraction patterns of both showed very similar changes.

Data were collected for these two derivatives to a resolution of 6 Å. As expected, the two difference Patterson maps showed essentially the same features.

In the first instance, one site (A) was put into each of the refinements, and $(F_o - F_c)e^{i\alpha_{FHLE}}$ maps calculated. The $UO_2F_5^{3-}$ map clearly indicated a second site (B) but, surprisingly, the $UO_2(CH_3COO)_2$ map did not, and attempts to impose one did not succeed. Subsequently, $(F_{PH} - F_P)e^{i\alpha_{iso}}$ maps were to confirm that, in spite of the similarity between the Patterson maps, there is only one site in $UO_2(CH_3COO)_2$ but two in the $UO_2F_5^{3-}$ derivative. The results of refinement are given in table 2.

Best phases were calculated by using the above parameters, the overall figure of merit being 0.66 (E' taken as $\frac{1}{2}E_{iso}$). The molecule appeared very similar to that in the tetragonal cell, and, in the light of the high-resolution interpretation of the latter, it was possible to trace the molecular backbone in the map.

TABLE 2. RESULTS OF REFINEMENT

(Abbreviations and symbols: h.a., heavy atom group; K, scale factor; O_c, relative occupancy; X, Y, Z are fractional coordinates; B, temperature factor (not refined); E, total standard error in closure of the isomorphous phase triangle (refined); $R = \Sigma||F_o|-|F_c||/\Sigma|F_o|$.)

h.a.	site	K	O_c	X	Y	Z	B	E	R (%)
$UO_2F_5^{3-}$	1 site, A	1.078	1.391	0.015	0.161	0.048	20	—	38.5
†$UO_2F_5^{3-}$	2 sites, A	1.071	1.337	0.013	0.162	0.049	20	103	34.4
	B		0.297	0.313	0.362	0.004	20		
†UO_2Ac_2	1 site, A	1.046	0.952	0.010	0.161	0.051	20	96	42.5

† Parameters used for phasing.

(*d*) *Molecular replacement* (For definition of symbols see table 1*b*.)

Because of the early difficulties encountered in finding heavy atom derivatives, a molecular replacement method was independently applied at 6 Å resolution. A hen egg-white lysozyme molecule from the tetragonal form was used as an isostructural model.

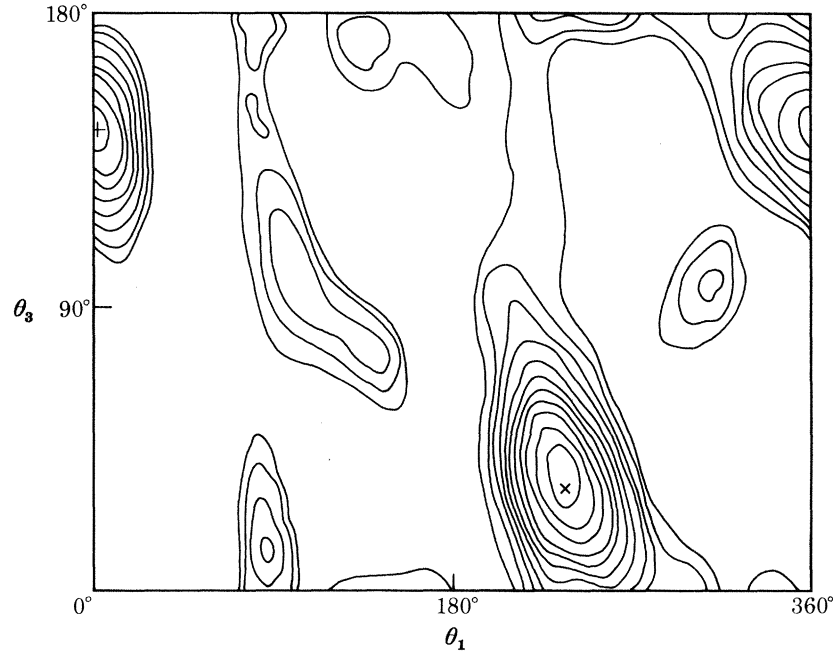

FIGURE 1. Section ($\theta_2 = 67°$) through the highest peak in the asymmetric unit of the Eulerian cell given by the rotation function $R(\boldsymbol{\theta})$, with use of the A model against B data at 6 Å. The rotation space group was $P2_1ab$. The best orientation is indicated by × ; + indicates the next highest peak. Eleven equidistant contours between the mean and maximum values are shown.

The rotation function $R(\boldsymbol{\theta})$ (Rossmann & Blow 1962; Crowther 1972) was evaluated from the complete set of independent reflexions F_0^2 of the orthorhombic form (B) over the range 25–6 Å and from $|F_m|^2$ calculated for the isolated model structure placed in a hypothetical P_1 cell with $a = b = c = 60$ Å and $\alpha = \beta = \gamma = 90°$ (Lifchitz 1983). The sampling interval was 5° for each Eulerian coordinate. The highest peak in the $R(\boldsymbol{\theta})$ map (figure 1) is 4.3 standard deviations above the mean value and is located at $\boldsymbol{\theta}_0 = (240°, 67°, 35°)$ and this specifies the orientation of the A molecule in the B cell. The next highest peak (three standard deviations above the mean value) lies in the same section $\theta_2 = 67°$ and may be explicable in terms of an approximate and fortuitous twofold symmetry in the lysozyme molecule at very low resolution.

A translational search was then made by applying the three-dimensional function $T(\boldsymbol{t})$, described in detail by Harada *et al.* (1981), with use of the same set of observations as for the determination of $\boldsymbol{\theta}_0$. The main peak in the $T(\boldsymbol{t})$ map led to solution $\boldsymbol{t}_0 = (0.891, 0.984, 0.531)$ for the translation of the rotated A molecule into the B cell. For ease of interpretation, it was found convenient to derive from $\boldsymbol{t}_0$ the vector $\boldsymbol{\tau}_0 = (0.772, 0.274, 0.104)$ which gives the position of the centre of mass of the molecule in the B cell: this is not far from $\frac{3}{4}, \frac{1}{4}$ in the C projection.

An $F_0 e^{i\alpha_c}$ map was calculated, the phases being obtained from $\boldsymbol{\theta}_0$ and $\boldsymbol{\tau}_0$ above. This map was compared with the $F_0 e^{i\alpha_{iso}}$ map from the double isomorphous replacement technique described above: the orientations of the molecules were generally very similar as were their positions relative to the symmetry axes. However, there were some observable orientational and positional discrepancies: it was evident that the six independent parameters from molecular replacement required refinement.

The third stage was therefore a low-resolution rigid body refinement by means of the local program ARTEMIS† (on an I.B.M. 370/165 computer) in Paris. This allows orientation, translation, overall B and scale factor to be refined either simultaneously or separately. The results of this refinement can be summarized as follows.

(i) The residual $R = \Sigma|F_o - F_c|/\Sigma F_o$ had an initial value of 52% for the 298 reflexions corresponding to 6 Å $< d <$ 10 Å. The scale factor had been refined and a B of 15 Å^2 adopted as indicated by a Wilson plot.

(ii) After three cycles of refinement, R had been reduced to 36% and the refined parameters were

$$\boldsymbol{\theta} = (237.3°, 66.1°, 29.9°), \boldsymbol{t} = (0.782, 0.283, 0.091), B = 19 \text{ Å}^2.$$

The parameter shifts in the refinement were approximately $\Delta\theta = 6.8°$ and $\Delta t = 1$ Å. This $\Delta\theta$ of nearly 7° corresponds to a deplacement of about 3 Å for peripheral atoms: this rotation and the Δt of 1 Å are half or less of the resolution (6 Å). This confirmed the validity and accuracy of molecular replacement in this case.

† ARTEMIS, written in Fortran, is available on request from A.L. It has also been deposited in the archives of the Royal Society and in the British Library, Lending Division; copies of the material deposited may be purchased from the British Library, Lending Division, Boston Spa, Wetherby, West Yorkshire LS23 7BQ, U.K. (reference SUP 10037).

These low-resolution refined atomic coordinates constituted the starting model for the restrained least squares refinements at 2.5 and 2.0 Å resolution.

(*e*) *Refinements*

(i) 2.5 Å *refinement*

The model obtained from the 6 Å rigid body refinement was used to calculate structure factors to 2.5 Å resolution. This gave a relatively low starting R factor at that resolution of 39.6%. The high-resolution refinement was done by means of the Hendrickson–Konnert restrained structure factor least squares program (Konnert 1976; Konnert & Hendrickson 1980) on the Oxford University I.C.L. 2980 computer and later on the CRAY-1 computer at the S.E.R.C. laboratory at Daresbury.

The progress of the 2.5 Å refinement is shown in table 3. Restraints were imposed not only on covalent bond lengths, covalent angles, planarities and chiralities, but also on hydrogen bonds and van der Waals contacts to prevent excessively close contacts. It is important to note that these last two restraints only model the repulsive and not the attractive part of the interaction; such contacts may therefore be broken and made in the course of the refinement. The hydrogen-bond pattern of the tetragonal lysozyme model was thus not imposed on the high-temperature orthorhombic model. There were 4476 structure factor observations, 1001 atoms, 2770 covalent distance restraints (including those defining angles), 179 planarities, 143 chiralities and 8775 possible contacts. An overall B factor of 19 Å^2 was adopted since it was felt that there were not enough observations to permit the refinement of individual atomic B factors at this resolution. Unit weights on F were employed. Terms from ∞ to 10 Å were omitted from refinement because in that range $F_c \gg F_o$, a result of the failure to describe the disordered solvent in the model. These terms are also not present in the R factors discussed below, unless otherwise stated.

After five cycles the refinement appeared to have converged to an R of 34.8% and the geometry had improved with only 154 covalent distances more than 0.02 Å from ideality compared with 566 at the beginning.

A $(3F_o - 2F_c)\,e^{i\alpha_c}$ map was calculated with use of the new model. A cursory examination of it revealed that most atoms were correctly situated in density but no reinterpretation or rebuilding was attempted because 2.0 Å data had become available, increasing the number of structure factor observations to 7386.

(ii) *First* 2.0 Å *refinement*

The first refinement at 2.0 Å resolution is summarized in table 3. The increased number of covalent distances deviating more than 0.02 Å from ideality, compared with the end of the 2.5 Å refinement, is due to the adoption of a new, slightly different dictionary of standard restraints in the interim. Eight cycles of refinement reduced R from 38.2 to 27% with, however, rather less tight restraints than previously. It was then decided to refine individual isotropic atomic B factors. These were unrestrained except for arbitrarily fixed maximum and minimum permitted values of 100 Å^2 and 5 Å^2. Because the disordered solvent affects the

TABLE 3. REFINEMENT TABLE

($R_{in} = \Sigma|F_o - F_c|/\Sigma F_o$ for the input model: N_{in}, number of distances >0.02 Å from ideality in the input model; S, scale factor F_c to F_o; $\langle B \rangle$, mean B for input model; Δr, ΔB, root mean square shifts on position and B values including damping factor; r.l. (l.), r.l. (h.), low and high resolution limits.)

	cycle	R_{in} (%)	N_{in}	S	$\langle B \rangle$ Å²	Δr Å	ΔB Å²	r.l. (l.) Å	r.l. (h.) Å
2.5 Å refinement	1	39.6	566	3.36		0.28			
	2	35.9	526	3.41	19.0	0.12	not		
	3	35.6	154	3.26	overall	0.07	refined	10	2.5
	4	35.3	197	3.26	value	0.04			
	5	34.8	154	3.26		0			
2.0 Å refinement I	1	38.2	388	3.35		0.10			
	2	34.6	131	3.20		0.10			
	3	30.3	222	3.20	15.9	0.09			
	4	29.3	211	3.20	overall	0.09	not	10	2.0
	5	27.8	234	3.21	value	0.07	refined		
	6	27.4	229	3.22		0.06			
	7	27.2	236	3.22		0.05			
	8	27.1	254	3.23		0.04			
	9	32.6	250	3.23	15.9	0.10	7		
	10	27.2	226	3.20	13.7	0.08	10		
	11	25.5	228	3.29	15.6	0.06	4	5	2.0
	12	24.5	235	3.36	16.6	0.05	10		
	13	24.1	226	3.40	–	0.05	15		
	14	23.8	234	3.41	–	0.09	0		
model rebuilt on graphics									
2.0 Å refinement II	1	31.8	261	3.30	17.0	0.06	5.2		
	2	28.5	208	3.24	14.5	0.02	2.1		
	3	26.7	217	3.37	14.7	0.03	1.4		
	4	26.0	213	3.41	15.1	0	1.1		
	5	25.6	213	3.46	15.5	0.01	1.4		
	6	25.3	220	3.49	15.9	0.01	0.8		
	7	25.1	222	3.53	16.3	0.04	0.9	5	2.0
	8	24.8	227	3.58	16.9	0.04	1.0		
	9	24.4	263	3.64	17.6	0.08	0.4		
	10	24.1	286	3.64	17.8	0.02	0.6		
	11	23.9	292	3.69	18.1	0.02	0.7		
	12	23.7	300	3.75	18.6	—	—		

intensities of reflexions with spacings > 5 Å (Artymiuk *et al.* 1983) and tends to have an adverse effect on P factor refinement, only data from 5 to 2.0 Å were used. The R factors quoted are thus not directly comparable with those given above. A further six cycles were then performed, which reduced R to 23.9%. This model was then used to calculate structure factors for *all* the data, including the low-resolution terms: the overall R was now 28.2%.

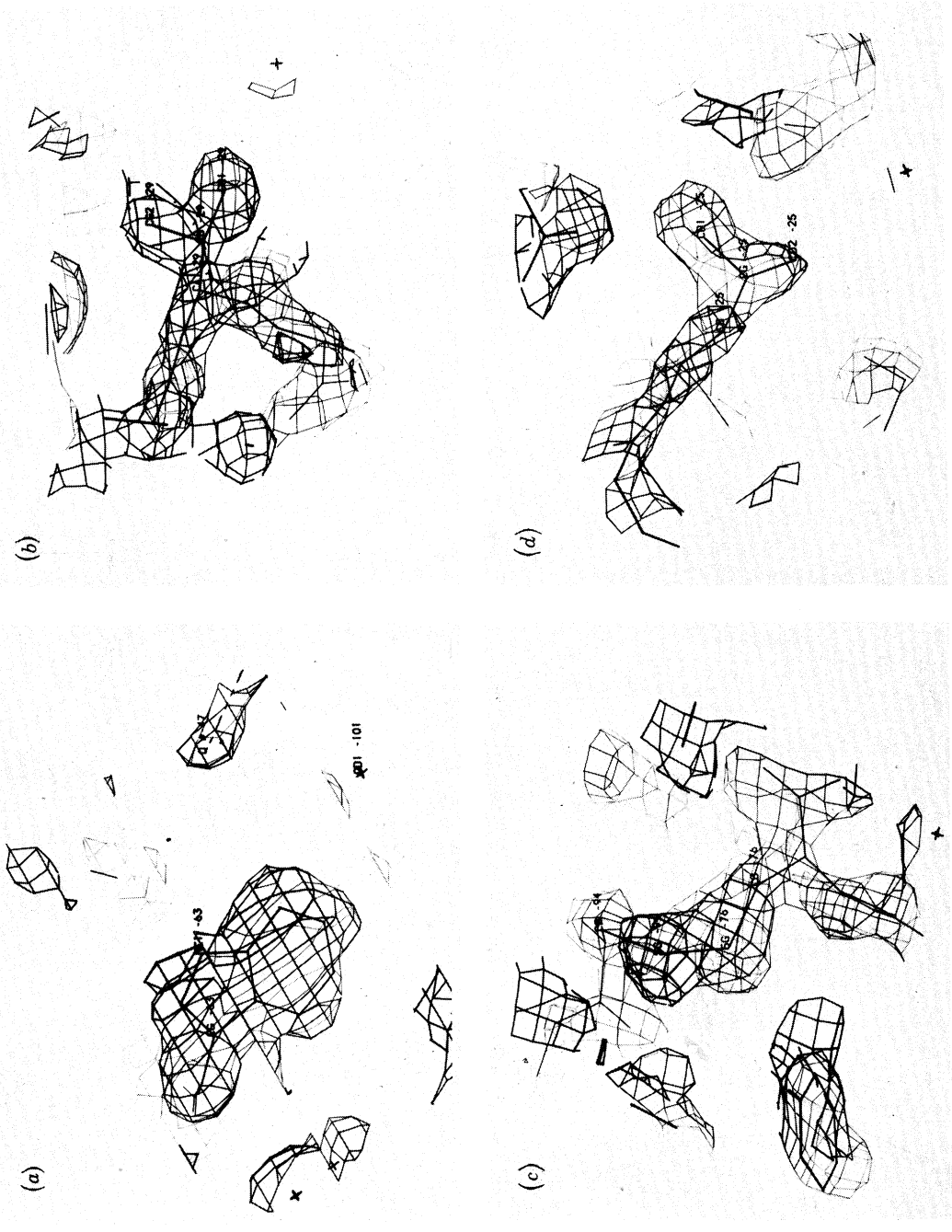

FIGURE 2. Electron density for characteristic side chains in the 2.0 Å resolution $(3F_o-2F_c)e^{i\alpha_c}$ map, calculated at the final stage of refinement. The contour level is 0.35 e Å^{-3}. Residues are shown are (*a*) Trp 63, (*b*) Val 29, (*c*) the Cys 76–Cys 94 disulphide bridge and (*d*) Leu 25.

(iii) *Rebuilding the model*

The structure factors were then used to calculate a $(3F_o - 2F_c)\,e^{i\alpha_c}$ map. This was examined on the S.E.R.C. Evans and Sutherland graphics system in the Laboratory of Molecular Biophysics, Oxford.

In general the map appeared very good; examples of typical residues are shown in figure 2. Where no density was observable for side chains this was generally also the case in tetragonal hen egg-white lysozyme (e.g. Lys 13 and Arg 14) and presumably can be attributed to disorder or mobility rather than to errors in the map. Elsewhere corrections were indicated to side-chain orientations that argued against any high degree of feedback from the model used to calculate the phases into the map.

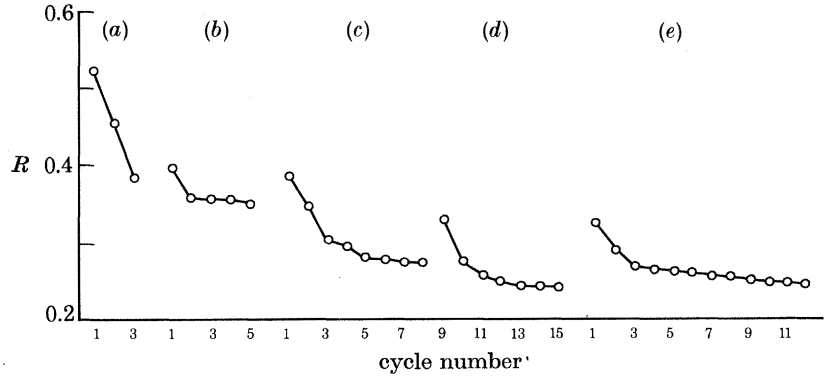

FIGURE 3. Progress of the refinement of high-temperature lysozyme. The R factor $R = \Sigma|F_o - F_c|/\Sigma F_o$ after each cycle of refinement is shown: (*a*) rigid body 6 Å refinement $10 \rightarrow 6$ Å; (*b*) 2.5 Å restrained structure factor least square (s.f.l.s.) refinement $10 \rightarrow 2.5$ Å; (*c*) first 2.0 Å restrained s.f.l.s. refinement $10 \rightarrow 2.0$ Å; (*d*) first 2.0 Å restrained s.f.l.s. refinement $5 \rightarrow 2.0$ Å; (*e*) second 2.0 Å restrained s.f.l.s. refinement $5 \rightarrow 2.0$ Å.

(iv) *Second* 2.0 Å *refinement*

After rebuilding, the refinement was resumed at 2.0 Å. This is summarized in table 3. The B factors were reset to an overall value of 17 Å^2 and refinement started again in a similar manner to before (see (ii) above). In 12 cycles, R was reduced from 31.8 to 23.7 % (the latter corresponding to 28 % on all data). This constituted no significant improvement on the previous 2.0 Å refinement; clearly the amount of rebuilding had been so small as to make little difference to the overall agreement of F_o and F_c. The overall progress of the refinement as monitored by the R factor is shown in figure 3.

At this stage no attempt was made to incorporate water molecules into the model, although density was visible at sites known from the tetragonal lysozyme refinement (D. E. P. Grace, D. C. Phillips, P. J. Artymiuk & H. Handoll, unpublished work). A more thorough examination of solvent structure will be possible when the refinement has been extended to 1.5 Å resolution.

3. Results and discussion

(*a*) *The map*

The map calculated from the refined model with coefficients $(3F_o-2F_c)\,e^{i\alpha_c}$ appears to be a good one: the peaks are sharp, carbonyls are distinct lobes of density, there are holes in the rings of some aromatic side chains (see for example Trp 63, figure 2), carboxyl groups are distinctly formed and so is the density for other branched side chains.

In tetragonal lysozyme five regions of the main chain are poorly ordered: Thr 47, Trp 62, Pro 70, Asp 101-Gly 102 and the C-terminal. Thr 47 has a very exposed side chain and the main-chain density for this residue was weak. In the orthorhombic form, the side chain is well defined, although the density for the α-carbon is weak.

The correct conformation of the loop 69–74 has provoked much discussion in the past: in the tetragonal crystals Grace (1979) obtained a refined map showing weak and indistinct density in this region; in the map of the chitotriose lysozyme complex (Blake *et al.* 1967*b*) the density is better ordered and in a different conformation. However, Kurachi *et al.* (1976) showed that in triclinic hen egg-white lysozyme yet another conformation is possible. The weak density for this region in the tetragonal crystals suggests that more than one conformation may exist in the crystals.

In the orthorhombic crystals, however, Thr 69, Pro 70, Gly 71, Ser 72 and Arg 73 form a generally well ordered loop, presumably because of a crystal contact (figure 4*a*). It is clear that Pro 70 is in the *trans*- and not the *cis*-conformation, although the density for the N and C_α of Gly 71 is weak. On the other hand residues Asp 101-Gly 102 are poorly defined in both the orthorhombic and tetragonal forms: in neither case are there any crystal contacts to stabilize this loop in any particular conformation.

So far as the side-chain density is concerned, Trp 62 is of interest. Its assignment in the upper part of the cleft has been carefully analysed in both tetragonal and triclinic lysozymes. In the tetragonal form, only the five-membered ring of the indole has a good density and this was taken to indicate librational motion about the C_β–C_γ bond (Blake *et al.* 1978). In the triclinic form, Kurachi *et al.* (1976) noticed this mobility of Trp 62 toward the bound inhibitor. In the orthorhombic crystal Trp 62 is, on the contrary, well located and strong density is present for the two rings of the indole group. When compared to its neighbour Trp 63 buried behind it, both tryptophans are equally well resolved (figure 4*b*); so it is unnecessary in this case to invoke a flapping motion about the C_β–C_γ bond. This is because of a crystal contact between the side chain of Trp 62 and residue 47 of a neighbouring molecule. A similar contact occurs in the unrelated room-temperature orthorhombic form of lysozyme (D. W. Rice, unpublished) where the indole ring of Trp 62 is also well ordered. In both crystal forms it has so far proved impossible to prepare chitotriose–lysozyme because of crystal shattering, presumably because of crystal contacts in the active site.

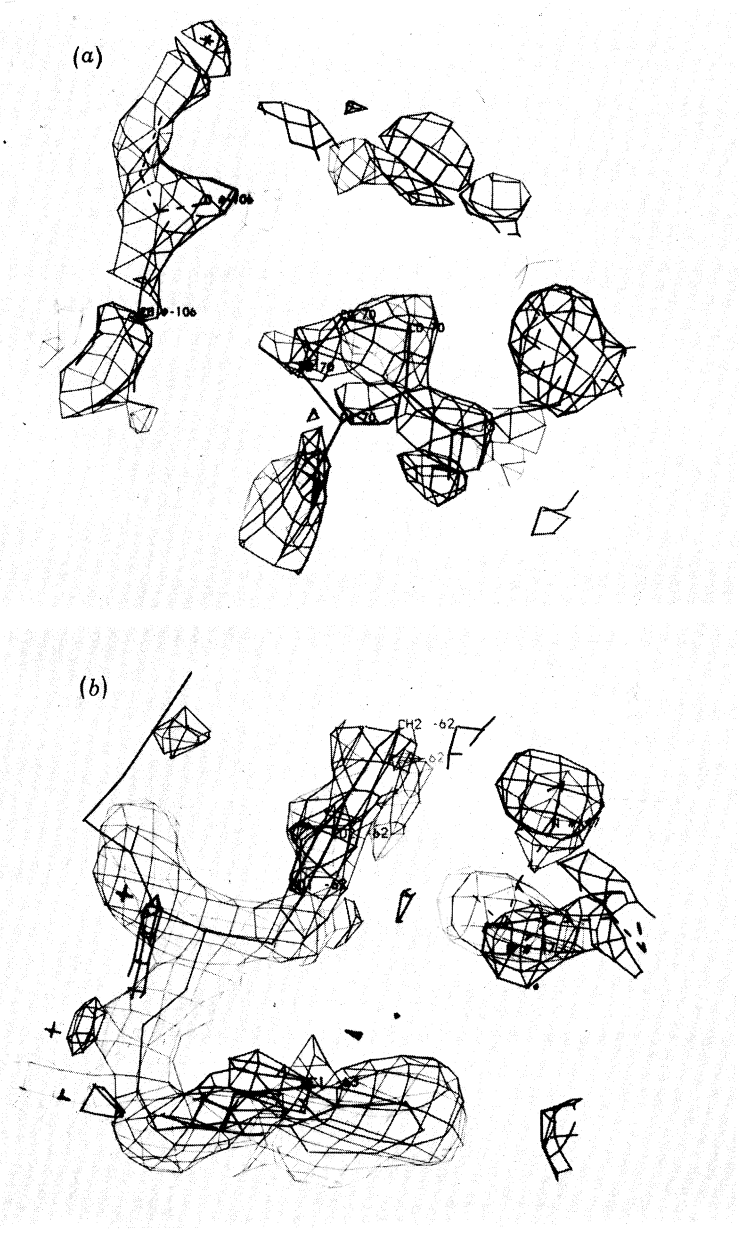

FIGURE 4. Densities from the $(3F_o-2F_c)e^{i\alpha_c}$ map for Pro 70 and Trp 62. The details of the map are the same as for figure 2. (*a*) Electron density in the vicinity of Pro 70 (centre). To the upper left side the density for residue 106 in a symmetry-related molecule can be seen. The 70 C_β–106 C_β distance is 3.62 Å; so these residues are in van der Waals contact. The proline side-chain density is well formed although the 70 C_α–70 C′ density is weak. (*b*) Electron density for the side chains of Trp 63 (bottom) and Trp 62 (upper centre). The density is well formed for both side chains. To the right, the density for residue 47 of a neighbouring molecule can be seen in van der Waals contact with Trp 62.

(*b*) *Comparison of coordinates with tetragonal hen egg-white lysozyme*

A least squares matrix was calculated to superimpose the α-carbon coordinates of tetragonal hen egg-white lysozyme (D. E. P. Grace, D. C. Phillips and P. J. Artymiuk, unpublished) onto those of high-temperature hen egg-white lysozyme.

The matrix found was such that

$$\tilde{\mathrm{M}}\begin{pmatrix} x \\ y \\ z \end{pmatrix}_{\text{tetragonal}} + \boldsymbol{t} = \begin{pmatrix} x \\ y \\ z \end{pmatrix}_{\text{orthorhombic}},$$

where

$$\tilde{\mathrm{M}} = \begin{pmatrix} -0.29447 & -0.83918 & 0.45724 \\ 0.56704 & 0.23171 & 0.79043 \\ -0.76926 & 0.049203 & 0.40761 \end{pmatrix}$$

and

$$\boldsymbol{t} = \begin{pmatrix} 52.32 \\ 1.40 \\ -15.55 \end{pmatrix}.$$

The root mean square deviations for α-carbon atoms was 0.464 Å and the variation along the chain is shown (figure 5). The maxima in this plot at residues 46–49, 70–74 and 101–102 and at the C-terminal residue (129) correspond essentially to the maxima in the *B* factor plots of the tetragonal form (figure 6*b*). This may indicate conformational differences in these poorly ordered loops or may simply reflect the difficulty in obtaining good coordinates in these areas of ill defined electron density.

If the rotation matrix is applied to all the coordinates the remaining differences greater than 1.0 Å occur for long hydrophilic sidechains such as Arg, Lys and Gln. This is not surprising: these are flexible groups on the outside of the molecule which are able to adopt different conformations in tetragonal and high-temperature orthorhombic lysozyme crystals, and indeed are often disordered.

The differences in the active site are not so large: for example the mean differences for the side chains of Trp 62 and Trp 63, important in stabilizing substrate binding, are 0.56 and 0.46 Å respectively, little more than the mean C_α discrepancy, while the differences for the catalytically important residues Glu 35, Asp 52 and Trp 108 are only 0.27, 0.15 and 0.23 Å respectively. There would thus appear to be no profound differences in the active sites of the two molecules.

(*c*) *Temperature factors*

Atomic motion causes the scattering power of an atom to fall off more rapidly with resolution than if the atom were stationary. The change in the scattering power is given by $e^{-B\sin^2\theta/\lambda^2}$, where *B*, the crystallographic temperature factor or *B* factor, can be related to the mean square amplitude of atomic displacement about the atom's mean position perpendicular to the reflecting planes, $\overline{U_\perp^2}$,

$$B = 8\pi^2\overline{U_\perp^2},$$

based on the assumption that the atom is engaged in isotropic harmonic motion in a quadratic potential well.

Because atomic thermal vibrations have frequencies of 10^{13} s^{-1} or less, they are slow compared with the X-ray frequencies of 10^{18} s^{-1}; it is not immediately possible to distinguish between thermal vibrations and static disorder. However, by collecting X-ray data at a variety of temperatures, refining the protein structures and comparing the resulting B factors, it is possible to distinguish between

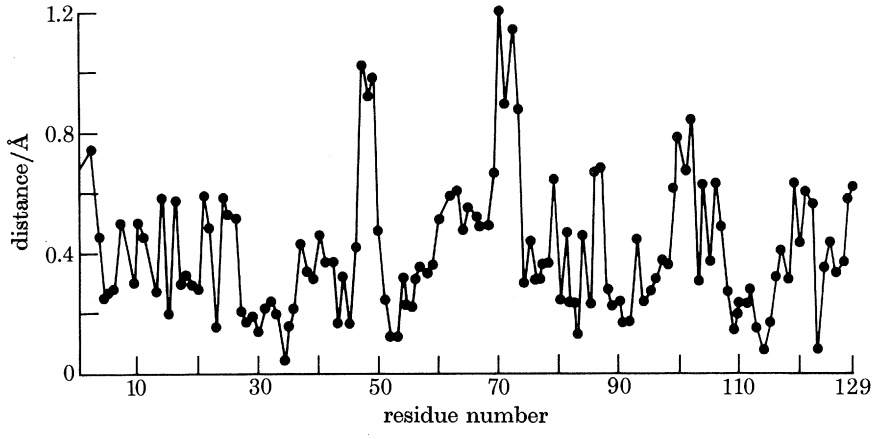

FIGURE 5. Plot of distance between equivalent superposed α-carbon atoms in high-temperature orthorhombic and tetragonal hen egg-white lysozyme against residue number after least squares superposition of α-carbon coordinates.

thermal vibrations (temperature-dependent) and static disorder (independent of temperature). Application of this method to the study of myoglobin suggests that real thermal vibrations are a major contribution to the B factor in protein crystals (Frauenfelder *et al.* 1979). In studies of orthorhombic human and tetragonal hen lysozyme it has been shown that there are strong similarities between the temperature factors of corresponding residues and that these correlate well with the secondary structure of the lysozyme molecule (Artymiuk *et al.* 1979). The average main-chain B factors for each residue in the high-temperature orthorhombic form are plotted in figure 6*a* and those for tetragonal hen egg-white lysozyme (D. E. P. Grace, D. C. Phillips and P. J. Artymiuk, unpublished) in figure 6*b*. The pattern of high-temperature factors around residues 47, 70 and 102 that can be seen in the tetragonal hen egg-white lysozyme graph has also been found to be characteristic of human lysozyme (Artymiuk *et al.* 1979). These three peaks correspond to loops in the structure that lie in the 'lips' of the active site of lysozyme. However, the high-temperature lysozyme graph does not show these peaks very strongly: the peak at residue 102 is still present but there are only relatively small upward trends near residues 47 and 70. This correlates with the fact that these residues are involved in contacts with symmetry-related molecules in the high-temperature orthorhombic crystals but not in the tetragonal ones, as has been noted in the discussion of electron density above. Examples of this are

shown in figure 4*a*, where the density of Pro 70 and Trp 62 residues is clear in the high- but not in the low-temperature form.

This may be interpreted in either of two ways: first, that crystal packing can substantially affect *B* factors in the crystals and cause regions that are mobile in solution or in other crystal forms to be held rigid by van der Waals contacts and hydrogen bonds or secondly that the transition from the low-temperature tetragonal form to the high-temperature orthorhombic form at 25 °C under otherwise

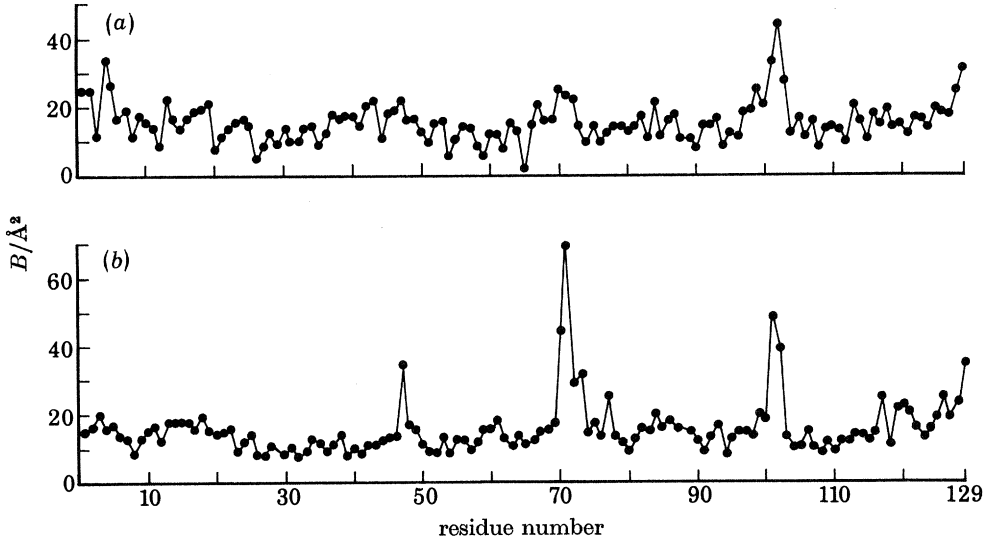

FIGURE 6. Plots of (*a*) mean main-chain temperature factors of high-temperature orthorhombic lysozyme against residue number; (*b*) mean main-chain temperature factors of tetragonal hen egg-white lysozyme against residue number.

identical conditions (Jollès & Berthou 1972; Berthou & Jollès 1974, 1978) is caused by a change in a major vibrational mode of the lysozyme molecule at around that temperature, and that the crystal packing has to change to accommodate it.

(*d*) *Hydrogen bond pattern*

Plots of the short (< 3.15 Å) main-chain NH to main-chain CO distances are shown in figure 7. They are plotted on a diagram based on that in Imoto *et al.* (1972). There do not seem to be any significant differences between the tetragonal and orthorhombic hydrogen-bonding patterns. Where differences appear, this is because in one molecule the appropriate distance is a little more than the 3.15 Å cut-off, and in the other a little less.

(*e*) *Ramachandran plot*

A Ramachandran plot for high-temperature orthorhombic hen egg-white lysozyme is shown in figure 8. All the non-glycine conformational angles lie in permitted areas of the plot, which shows the effectiveness of the refinement process in producing a stereochemically reasonable model.

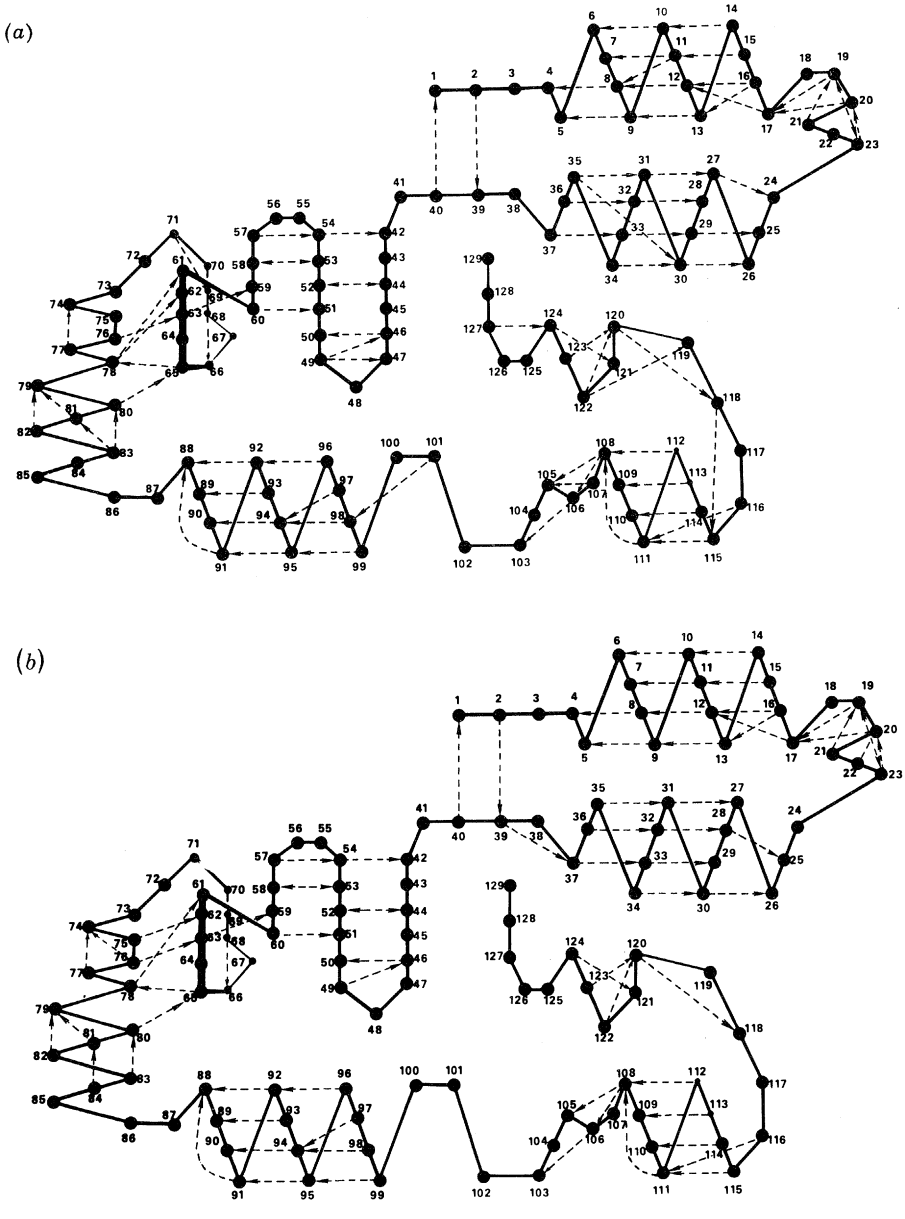

FIGURE 7. Hydrogen bonds NH···CO between groups in the main polypeptide chain in (*a*) orthorhombic high-temperature hen egg-white lysozyme; (*b*) tetragonal hen egg-white lysozyme. All main chain N···O contacts less than 3.15 Å are shown.

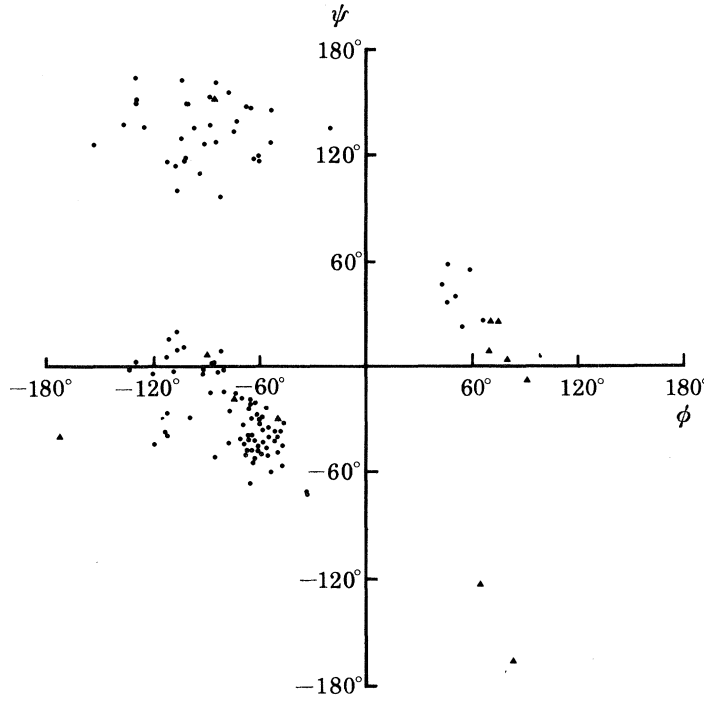

FIGURE 8. A Ramachandran plot of the high-temperature orthorhombic form of hen egg-white lysozyme from the final stage of refinement. Non-glycine residues are shown as filled circles and glycine residues as triangles.

4. CONCLUSIONS

The basis of this work has been the comparison of similar structures at similar levels of resolution. The structure of tetragonal lysozyme has served as a reference model.

Analyses of the map have shown that the conformations of the lysozyme molecule in the two crystal forms are very similar and the root mean square difference in coordinates of corresponding backbone is only 0.46 Å. We have found some appreciable local differences involving both the main chain and side chains on the surface. In general, these arise from the different modes of packing in the two crystal forms causing different regions of the protein to be involved in intermolecular contacts.

In spite of the difference in temperature of crystallization and the consequent difference in crystal form, the main structural features of the enzyme are preserved. It is evident that the changes responsible for the changes in the behaviour of the enzyme at physiological as opposed to room temperature are extremely subtle and may be defined only by further analysis at higher resolution.

This research was supported by the C.N.R.S. (LA no. 19 and ER no. 102), by I.N.S.E.R.M. (Unité U-116), by the University of Paris VI and by the United

Kingdom Medical Research Council (P.A.). We thank the Science and Engineering Research Council for the use of the Cray I computer at their Daresbury workstation. The authors are indebted to Dr B. Bachet and Dr D. W. Rice for assistance in collecting diffractometer data, to Mr A. Laurent for his help and advice and to Mrs M. Rougeot for skilful technical assistance.

We are grateful to Professor H. Curien and to Dr C. C. F. Blake for their continuing interest in this work and thank Professor Sir David Phillips, Sec.R.S., for his constant help and encouragement and for his comments on the manuscript of this paper.

References

Artymiuk, P. J., Blake, C. C. F., Grace, D. E. P., Oatley, S. J., Phillips, D. C. & Sternberg, M. J. E. 1979 Crystallographic studies of the dynamic properties of lysozyme. *Nature, Lond.* **280**, 563–568.

Artymiuk, P. J., Blake, C. C. F. & Pulford, W. C. A. 1983 In preparation.

Artymiuk, P. J., Blake, C. C. F., Rice, D. W. & Wilson, K. S. 1982 The structure of the monoclinic and orthorhombic forms of hen egg-white lysozyme at 6 Å resolution. *Acta crystallogr.* B **38**, 778–783.

Banner, D. W., Evans, P. R., Marsh, D. J. & Phillips, D. C. 1977 A multiple counter X-ray diffractometer with equatorial geometry. *J. appl. Crystallogr.* **10**, 45–51.

Berthou, J. & Jollès, P. 1974 A phase transition in a protein crystal: the example of hen lysozyme. *Biochim. biophys. Acta* **336**, 222–227.

Berthou, J. & Jollès, P. 1978 Extension of the transition phenomenon in hen egg-white lysozyme crystals: the case of the monoclinic crystals. *Biochimie* **60**, 209–210.

Berthou, J., Laurent, A., Lifchitz, A., Jollès, P., Artymiuk, P. & Rice, D. W. 1977 Structural study of the high temperature form of hen egg white lysozyme. 4th European Crystallography Meeting, Oxford.

Blake, C. C. F., Grace, D. E. P., Johnson, L. N., Perkins, S. J., Phillips, D. C., Cassels, R., Dobson, C. M., Poulsen, F. M. & Williams, R. J. P. 1978 Physical and chemical properties of lysozyme. Molecular interactions and activity in proteins, *Ciba Found. Symp.* **60**, 138–185.

Blake, C. C. F., Johnson, L. N., Mair, G. A., North, A. C. T., Phillips, D. C. & Sarma, V. R. 1967*b* Crystallographic studies of the activity of hen egg-white lysozyme. *Proc. R. Soc. Lond.* B **167**, 378–388.

Blake, C. C. F., Koenig, D. F., Mair, G. A., North, A. C. T., Phillips, D. C. & Sarma, V. R. 1965 Structure of hen egg-white lysozyme. A three-dimensional Fourier synthesis at 2 Å resolution. *Nature, Lond.* **206**, 757–761.

Blake, C. C. F., Mair, G. A., North, A. C. T., Phillips, D. C. & Sarma, V. R. 1967*a* On the conformation of the hen egg-white lysozyme molecule. *Proc. R. Soc. Lond.* B **167**, 365–377.

Blow, D. M. & Crick, F. H. C. 1959 The treatment of errors in the isomorphous replacement method. *Acta crystallogr.* **12**, 794–802.

Coppens, R., Leiserowitz, L. & Rabinovich, D. 1965 Calculation of absorption corrections for camera and diffractometer data. *Acta crystallogr.* **18**, 1035–1038.

Cozzone, P., Opella, S. J., Jardetzky, O., Berthou, J. & Jollès, P. 1975 Detection of a new temperature-dependent conformational transition in lysozyme by carbon-13 nuclear magnetic resonance spectroscopy. *Proc. natn. Acad. Sci. U.S.A.* **72**, 2095–2098.

Crowther, R. A. 1972 In *The molecular replacement method* (ed. M. G. Rossman), pp. 174–177. New York: Gordon and Breach.

Dodson, E. & Vijayan, M. 1971 The determination and refinement of heavy-atom parameters in protein heavy-atom derivatives. Some model calculations using acentric reflexions. *Acta crystallogr.* B **27**, 2402–2411.

Frauenfelder, H., Petsko, G. A. & Tsernoglou, D. 1979 Temperature-dependent X-ray diffraction as a probe of protein structural dynamics. *Nature, Lond.* **280**, 558–563.

Grace, D. E. P. 1979 A refined analysis of the structure of lysozyme and its interactions with the substrate. D.Phil. thesis, Oxford University.

Harada, Y., Lifchitz, A., Berthou, J. & Jollès, P. 1981 A translation function combining packing and diffraction information: an application to lysozyme. *Acta crystallogr.* A **37**, 398–406.

Hodson, J. M., Siecker, L. C. & Jensen, L. H. 1974 Am. Crystallogr. Ass. Spring Meeting, Abstract J8.

Hogle, J., Rao, S. T., Mallikarjunan, M., Beddell, C., McMullan, R. K. & Sundaralingam, M. 1981 Studies of monoclinic hen egg white lysozyme I. Structure solution at 4 Å resolution of molecular-packing comparisons with tetragonal and triclinic lysozymes. *Acta crystallogr.* B **37**, 591–597.

Imoto, T., Johnson, L. N., North, A. C. T., Phillips, D. C. & Rupley, J. A. 1972 In *The enzymes* (ed. P. D. Boyer), pp. 665–868. New York: Academic Press.

Jollès, P. & Berthou, J. 1972 High temperature crystallization of lysozyme: an example of phase transition. *FEBS Lett.* **23**, 21–23.

Jollès, P., Saint-Blancard, J., Allary, M., Perin, J.-P. & Cozzone, P. 1975 On the binding of *N*-acetylglucosamine and its short polymers to hen lysozyme at physiological temperature (40 °C). *FEBS Lett.* **55**, 165–167.

Joynson, M. A., North, A. C. T., Sarma, V., Dickerson, R. E. & Steinrauf, L. K. 1970 Low resolution studies on the relationship between the triclinic and tetragonal forms of lysozyme. *J. molec. Biol.* **50**, 137–142.

Konnert, J. H. 1976 A restrained-parameter structure-factor least-squares refinement procedure for large asymmetric units. *Acta crystallogr.* A **32**, 614–617.

Konnert, J. H. & Hendrickson, W. A. 1980 A restrained-parameter thermal-factor refinement procedure. *Acta crystallogr.* A **36**, 344–350.

Kurachi, K., Siecker, L. C. & Jensen, L. N. 1976 Structures of triclinic mono- and di-*N*-acetylglucosamine:lysozyme complexes. A crystallographic study. *J. molec. Biol.* **101**, 11–24.

Lifchitz, A. 1983 On the choice of the mode cell and the integration volume in the use of the rotation function. *Acta crystallogr.* A **39**. (In the press.)

Moult, J., Yonath, A., Traub, W., Smilansky, A., Podjorny, A., Rabinovich, D. & Saya, A. 1976 The structure of triclinic lysozyme at 2.5 Å resolution. *J. molec. Biol.* **100**, 179–195.

North, A. C. T., Phillips, D. C. & Mathews, F. S. 1968 A semi-empirical method of absorption correction. *Acta crystallogr.* A **24**, 351–358.

Rossman, M. G. & Blow, D. M. 1962 The detection of sub-units within the crystallographic asymmetric unit. *Acta crystallogr.* **15**, 24–31.

Saint-Blancard, J., Clochard, A., Cozzone, P., Berthou, J. & Jollès, P. 1977 The temperature dependent structural transition of lysozyme: a study of the Arrhenius plots. *Biochim. biophys. Acta* **491**, 354–356.

Saint-Blancard, J., Maurel, J. P., Constant, J. F., Berthou, J. & Jollès, P. 1981 Influence of pH and ionic strength on the lysis of *Micrococcus luteus* cells by hen lysozyme at low (20 °C) and high (physiological, 40 °C) temperature. *Biosci. Rep.* **1**, 119–123.

Saint-Blancard, J., Mazurier, J., Bournaud, M., Maurel, P. P., Berthou, J. & Jollès, P. 1979 The temperature and pH-dependent transition of hen lysozyme. Characterization of two temperature-defined domains and of a *N*-acetylglucosamine (inhibitor)-insensitive form. *Molec. Biol. Rep.* **5**, 165–169.

Steinrauf, L. K. 1959 Preliminary X-ray data for some new crystalline forms of β-lactoglobulin and hen egg-white lysozyme. *Acta crystallogr.* **12**, 77–79.

Watson, H. C., Shotton, D. M., Cow, J. M. & Muirhead, N. 1970 Three dimensional Fourier synthesis of tosyl elastase at 3.5 Å resolution. *Nature, Lond.* **225**, 806–813.

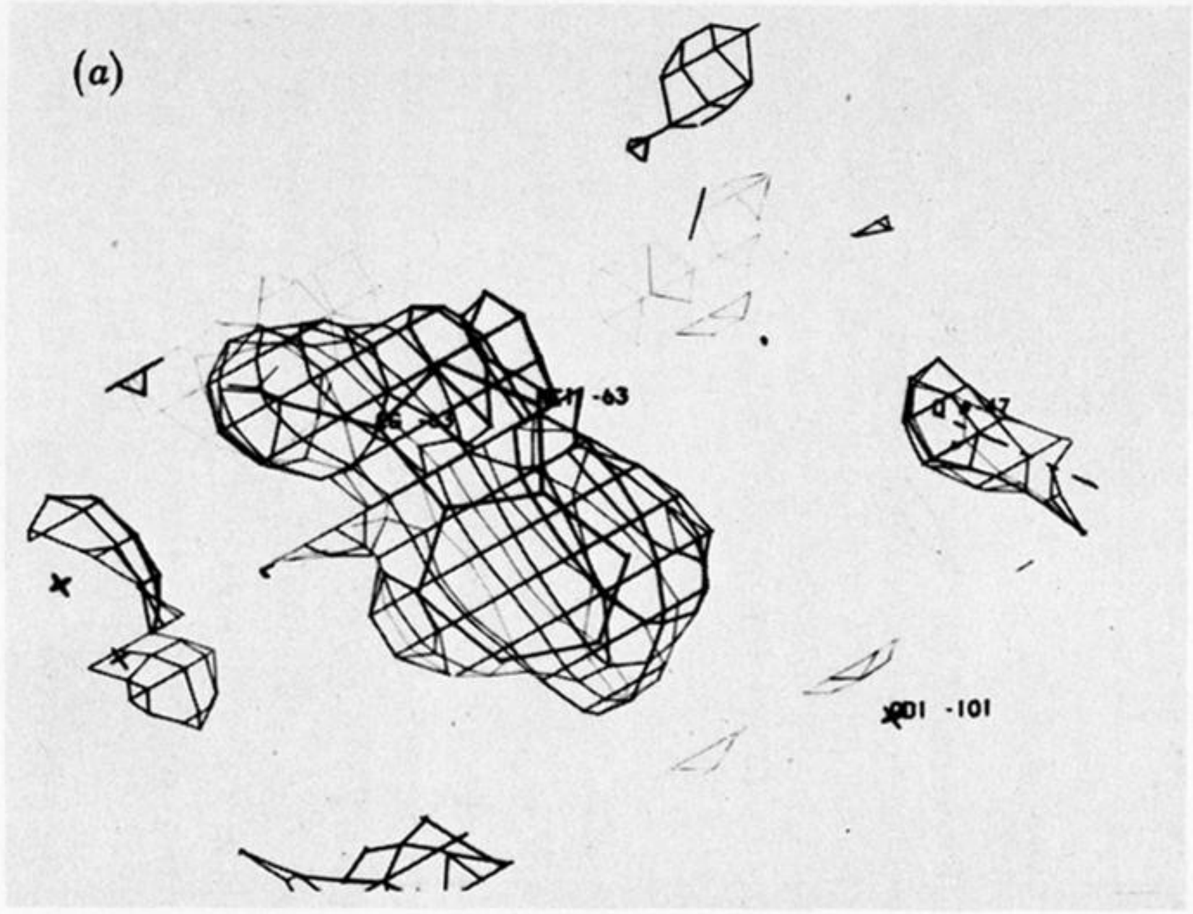

FIGURE 2. Electron density for characteristic side chains in the 2.0 Å resolution $(3F_o-2F_c)\,e^{i\alpha_c}$ map, calculated at the final stage of refinement. The contour level is 0.35 e Å^{-3}. Residues are shown are (*a*) Trp 63, (*b*) Val 29, (*c*) the Cys 76–Cys 94 disulphide bridge and (*d*) Leu 25.

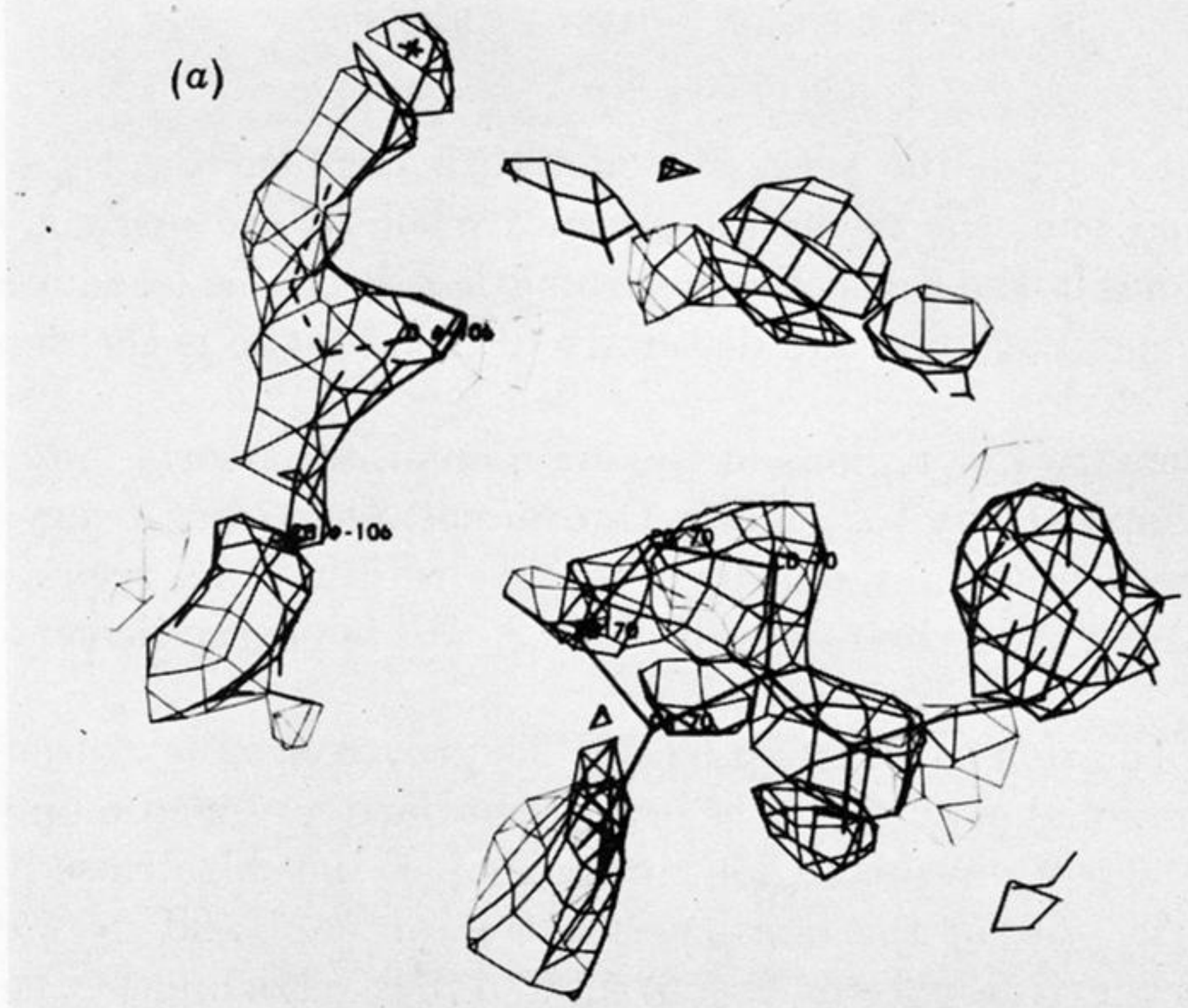

FIGURE 4. Densities from the $(3F_o-2F_c)\,e^{i\alpha_c}$ map for Pro 70 and Trp 62. The details of the map are the same as for figure 2. (*a*) Electron density in the vicinity of Pro 70 (centre). To the upper left side the density for residue 106 in a symmetry-related molecule can be seen. The 70 C_β–106 C_β distance is 3.62 Å; so these residues are in van der Waals contact. The proline side-chain density is well formed although the 70 C_α–70 C′ density is weak. (*b*) Electron density for the side chains of Trp 63 (bottom) and Trp 62 (upper centre). The density is well formed for both side chains. To the right, the density for residue 47 of a neighbouring molecule can be seen in van der Waals contact with Trp 62.